

CONSTRAINING BLACK HOLE FORMATION WITH 2M05215658+4359220

KATELYN BREIVIK,¹ SOURAV CHATTERJEE,² AND JEFF J. ANDREWS^{3,4}

- ¹*Canadian Institute for Theoretical Astrophysics, University of Toronto, 60 St. George Street, Toronto, Ontario, M5S 1A7, Canada*
²*Tata Institute of Fundamental Research, Division of Astronomy and Astrophysics, Homi Bhaba Road, Navy Nagar, Colaba, Mumbai, 400005, India*
³*Foundation for Research and Technology-Hellas, 100 Nikolaou Plastira St., 71110 Heraklion, Crete, Greece*
⁴*Physics Department & Institute of Theoretical & Computational Physics, P.O Box 2208, 71003 Heraklion, Crete, Greece*

ABSTRACT

We show that the recently discovered binary 2M05215658+4359220, comprised of a giant star (GS) orbiting a suspected black hole (BH) in a ~ 80 day orbit, may be instrumental in shedding light on uncertain BH-formation physics and can be a test case for studying wind accretion models. Using binary population synthesis and a realistic prescription of the star formation history and metallicity evolution of the Milky Way, we analyze the formation histories of detached BH–GS binaries like 2M05215658+4359220, and find that all such systems with orbital periods less than 5 years went through a common envelope. Furthermore, the ‘rapid’ and ‘delayed’ supernova engine models produce very different BH mass distributions in BH–GS binaries, and one current mass estimate for the BH in 2M05215658+4359220 is inconsistent with the rapid model. An improved measurement of the orbit of 2M05215658+4359220, which we argue is imminent with the next *Gaia* data release, therefore has widespread implications including for SN engine models and for the types of binaries detectable by LIGO and LISA. Finally, we show that the reported X-ray non-detection is a challenge for wind accretion theory, making 2M05215658+4359220 a prime target for further study with accretion models.

Keywords: black hole physics—methods: numerical—astrometry—binaries: general—stars: black holes—X-rays: binaries

1. INTRODUCTION

Recent discoveries of merging binary black holes (BBHs) by the LIGO-Virgo observatories (e.g., Abbott et al. 2016a,b, 2017a,b,c) have reignited widespread interest in the astrophysical origins of these sources. One of the major uncertainties in interpreting the observational results as well as creating predictive models for the BBH merger rate and the distribution of expected BBH properties can be directly attributed to the lack of constraints on quantities related to BH-formation physics, such as their mass function and kick distribution at birth (e.g., Chatterjee et al. 2017). Theoretical modeling of the death throes of a massive star is notoriously difficult, and numerical simulations are not yet at a stage to provide strong constraints without observations (e.g., Fryer et al. 2012; Belczynski et al. 2012; Woosley 2017; Burrows et al. 2018). On the other hand, dark remnants are challenging to discover, hence, it is hard to infer strong constraints from the limited number of stellar BHs, identified primarily in accreting systems via X-ray and radio emissions (e.g., Gallo et al. 2014; Corral-Santana et al. 2016). Thus, finding and characterizing BHs is highly important for several branches in astrophysics.

In addition to small detection numbers, the distribution of properties also suffers from severe selection biases. Traditionally, only BHs in mass-transferring systems could be detected via their X-ray and radio emissions, and there is strong bias towards detecting distant massive BHs via gravitational wave (GW) detectors such as LIGO/Virgo (e.g., Messenger & Veitch 2013). The possibility of identifying BHs in detached binaries with luminous companions (LC) was discussed nearly 50 years ago by Trimble & Thorne (1969), who provide a list of single-line spectroscopic binaries with large radial velocity (RV) variations. Modern applications of this method have recently discovered BH candidates in detached binary systems in both a star cluster (Giesers et al. 2018) and the field (Thompson et al. 2018, henceforth T18).

The BH detection methods discussed above present challenges, since each detection is observationally expensive, typically requiring significant time on large-aperture telescopes. As an alternative, for nearby systems with large orbits, the astrometric motion of the LC can provide stringent constraints on the system (e.g., Sirius; Bond et al. 2017). Recently, it has been demonstrated by several groups that the astrometric mission *Gaia* can use this method to identify BHs in detached orbits with LCs (Barstow et al. 2014; Mashian & Loeb 2017; Breivik et al. 2017; Yamaguchi et al. 2018; Yalinewich et al. 2018). While the studies disagree on the expected yield of detached BH-LC binaries during the nominal *Gaia* survey duration, they all agree that such binaries exist and that *Gaia* should detect them. Furthermore, they agree that variations in BH-formation

physics lead to observable differences in the population of BH-LC binaries expected to be discovered by *Gaia*. Hence, with a large enough sample, *Gaia* can constrain details of the BH-formation process (Breivik et al. 2017). Most recently, it has also been suggested that BH-LCs in detached systems may also be discovered via photometric variations of the LCs using, for example, *TESS* data (Masuda & Hotokezaka 2018). *Gaia* and *TESS* probe a very different parameter space compared to that covered by X-ray, radio, or GWs; the astrometric detection of stellar BHs is therefore an exciting prospect for both increasing the known population, as well as exploring a different region of parameter space for BH binaries (Breivik et al. 2017).

The recent discovery by T18 that 2M05215658+4359220 is a giant star (GS) companion to a dark remnant in a 83.2-day orbit, presents the strongest case to date for BH-LC binaries in the field of the Milky Way (MW). T18 demonstrated that RV and photometric measurements of 2M05215658+4359220 show a matching periodicity indicative of tidal locking between the binary orbit and the spin of the GS. These assumptions, combined with a spectroscopic measurement of the rotational velocity and a parallax distance measurement from *Gaia* allow T18 to constrain $\sin i$, typically unknown in RV measurements. Based on these assumptions, T18 estimate the dark companion’s mass to fall within the range $2.5 < M_{\text{rem}}/M_{\odot} < 5.8$. The mass derivations in T18 suggest the possibility of 2M05215658+4359220’s companion being a BH that falls within the observed ‘mass gap’ region for BHs with masses $\lesssim 5 M_{\odot}$ (Özel et al. 2010; Farr et al. 2011). Given these constraints, 2M05215658+4359220 may be the first of a completely new class of BH binaries soon to be discovered by *Gaia*.

The primary goal of this paper is to understand in detail the astrophysical formation channel for detached BH binaries similar in properties to 2M05215658+4359220 and investigate the potential for 2M05215658+4359220 to place constraints on BH formation in binary systems. In Section 2 we describe our population synthesis code used to generate populations of binaries formed in the MW. In Section 3 we describe the dominant formation channels for BH binaries with properties similar to those of 2M05215658+4359220 and discuss how 2M05215658+4359220 may be used to constrain BH formation. In Section 4, we discuss this system in the context of *Gaia*’s observational capabilities and wind accretion models. We finish with a summary of our key results in Section 5.

2. SIMULATING MILKY WAY’S BH BINARIES

We use the population synthesis code *cosmic*¹ to simulate a realistic MW population of binaries consisting of BHs orbiting GSs (BH-GS; Breivik et al. 2017). We

¹ <https://cosmic-popsynth.github.io/>

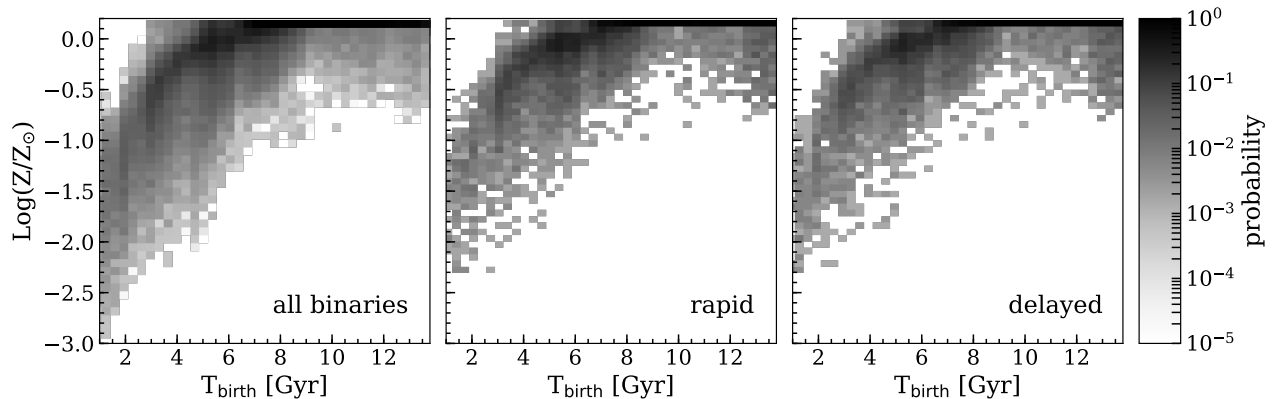


Figure 1. Distributions of birth time and metallicity based on galaxy **m12i** in the Latte simulation suite (see text). The left-most panel shows the distribution from **m12i**. The middle and right panels show the same for simulations initialized to $T_{\text{birth}} = 0$, for the populations of BH–GS binaries at present epoch from the rapid and delayed SN models.

adopt a metallicity-dependent MW star formation history, as done in [Lamberts et al. \(2018\)](#), based on galaxy **m12i** in the Latte simulation suite². [Figure 1](#) shows the metallicity and birth time of all stars formed in the **m12i** model, as well as the same distributions for BH–GS systems at present epoch for the two binary populations we create using different prescriptions based on the supernova (SN) engine models from [Fryer et al. \(2012\)](#).

One SN-engine model (‘rapid’) produces a mass gap between BHs and neutron stars (NSs) and the other (‘delayed’) does not. The rapid model assumes strong convection which allows instabilities to grow quickly (within ~ 250 ms) after core bounce, producing fewer but more energetic SN explosions and BHs with higher masses. The delayed model, on the other hand, allows convective instabilities to grow over a wider range of timescales leading to a continuous distribution of remnant masses.

We assume standard parameter distributions to initialize our binary population. Initial primary masses are distributed according to [Kroupa \(2001\)](#), and we use a primary-mass-dependent binary fraction ([van Haaften et al. 2013](#), and references therein). Secondary masses are drawn from a flat distribution in mass ratios between 0.001 and 1 (e.g., [Mazeh et al. 1992](#)). Orbital periods (P_{orb}) are distributed uniformly in log-days ([Abt 1983](#)), where the upper bound is $10^5 R_{\odot}$ and the lower bound is set such that the primary star’s radius is less than half of the Roche-lobe radius. We assume a thermal initial eccentricity (e) distribution ([Heggie 1975](#)).

`cosmic` uses the binary stellar evolution code `BSE` ([Hurley et al. 2002](#)) to evolve an initialized population of binaries to the present day. We note that `BSE` limits

binary metallicities to be between $0.005 < Z/Z_{\odot} < 1.5$, thus we force all metallicities taken from **m12i** to fall within this range. To scale our simulations to the MW, we track the total simulated mass including single and binary stars in our populations (M_{tot}). We then scale the number of BH–GS binaries by $M_{\text{FIRE}}/M_{\text{tot}}$, where $M_{\text{FIRE}}/M_{\odot} = 2.7 \times 10^{10}$ is the total mass of stars formed in galaxy **m12i**.

We assume that BHs are born with a natal kick drawn from a Maxwellian distribution with $\sigma = 265$ km/s ([Hobbs et al. 2005](#)), which is then reduced by the fraction of ejected mass that falls back onto the BH during formation ([Fryer et al. 2012](#)). We employ the $\alpha\lambda$ common envelope (CE) prescription where $\alpha = 1.0$ is the CE efficiency and λ is the non-dimensional binding energy of the stellar envelope, determined with the default `BSE` prescription ([Claeys et al. 2014](#), see their appendix).

3. RESULTS

3.1. Formation Channels

We select the subset of all simulated BH–GS binaries that are similar to 2M05215658+4359220 ($0.5 \text{ day} < P_{\text{orb}} < 5 \text{ yr}$ and $e = 0$) for both SN prescriptions, and outline their evolutionary formation and branching ratios in [Figure 2](#). The majority of our BH–GS systems at present day have super-solar metallicities (80% and 83% for the rapid and delayed models) and thus have suffered strong line-driven stellar winds ([Vink et al. 2001](#)). This leads to a maximum BH mass of $M_{\text{BH}}/M_{\odot} \simeq 10$ for systems which experience a CE and $M_{\text{BH}}/M_{\odot} \simeq 24$ overall. Although the vast majority of BH–GS binaries evolve without significant interaction, such systems have wide orbits; all BH–GS binaries with $P_{\text{orb}}/\text{yr} < 5$ have undergone a CE regardless of the SN engine.

[Figure 2](#) also shows that the rapid model produces fewer, but more massive BHs than the delayed model for the reasons detailed in [Section 2](#). Systems evolved

² The Latte suite of FIRE-2 cosmological, zoom-in, baryonic simulations of MW-mass galaxies ([Wetzel et al. 2016](#)), part of the Feedback In Realistic Environments (FIRE) simulation project, were run using the Gizmo gravity plus hydrodynamics code in meshless, finite-mass mode ([Hopkins 2015](#)) and the FIRE-2 physics model ([Hopkins et al. 2018](#))

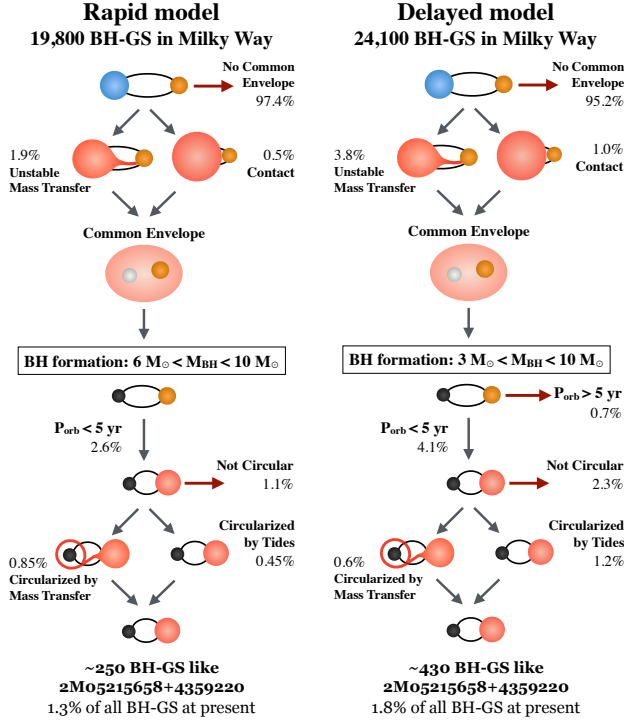


Figure 2. Evolutionary channels to form BH-GS binaries similar to 2M05215658+4359220, with relative rates of each evolutionary stage. Systems from both the rapid and delayed models begin as massive stars with a lower mass stellar companion. The majority of BH-GS progenitors have super-solar metallicities and thus strong stellar winds which limit the final BH mass distribution. All formation scenarios that produce BH-GSs similar to 2M05215658+4359220 predict that the system undergoes a CE, followed by a SN which produces a BH. The BH companion then evolves off of the main sequence and the orbit can either remain eccentric or circularize. We deem a BH-GS to be similar to 2M05215658+4359220 if it has $P_{\text{orb}}/\text{yr} < 5$ and $e = 0$.

with the delayed model are limited to a lower bound of $3 M_{\odot}$ (chosen as the mass separating NSs from BHs), while the rapid model only produces BH masses in excess of $\approx 5 M_{\odot}$. This is particularly important given the low BH masses ($\sim 2-5 M_{\odot}$) derived in T18. For systems which undergo a CE, the lower BH masses produced by the delayed model receive higher natal kicks and are thus more likely to be found in high- e and longer- P_{orb} binaries when compared to the rapid model. Nevertheless, we find that the delayed model produces about twice as many 2M05215658+4359220-like BH-GS binaries.

Black contours in Figure 3 show the distribution of P_{orb} and BH masses for all simulated BH-GS binaries. We overplot the two mass measurements of the dark companion to 2M05215658+4359220 made by T18. One measurement combines spectroscopic RVs, $\log g$ and T_{eff} with MIST single star models, which produces mass con-

straints of $M_{\text{rem}}/M_{\odot} \simeq 3.2^{+1.1}_{-0.4}$ and $M_{\text{GS}}/M_{\odot} \simeq 3.0^{+0.6}_{-0.5}$ (orange error bars). A second, similar fit leaves $\log g$ as a free parameter which produces mass constraints of $M_{\text{rem}}/M_{\odot} \simeq 5.5^{+3.2}_{-2.2}$ and $M_{\text{GS}}/M_{\odot} \simeq 2.2^{+1.0}_{-0.9}$ (black error bars). While the P_{orb} measurements from T18 are consistent with the bulk of our simulated systems from both models, only the higher inferred remnant mass is consistent with the BH masses in the rapid model.

Both SN prescriptions produce populations of BH-GS binaries with $P_{\text{orb}}/\text{yr} \lesssim 5$, which coincides with the region of *Gaia*'s sensitivity (bounded by the blue vertical lines). Note that the true lower-period cutoff for *Gaia*'s sensitivity is dependent on the binary's distance and orientation, as well as the sky-position-dependent cadence of observation. Nevertheless, the ≈ 83 day orbit of M05215658+4359220 is within *Gaia*'s limits even by conservative estimates.

The distribution of BH-GS systems in Figure 3 at larger P_{orb} either avoided a CE during their formation or had their orbits lengthened by BH natal kicks (found in delayed model). Therefore, the population of BH-GS binaries similar to 2M05215658+4359220, and, more broadly, to which *Gaia* is sensitive, are exclusively made up of post-CE systems.

3.2. Using 2M05215658+4359220 to constrain BH formation models

Figure 4 compares the masses of our simulated BH-GS populations (blue and orange contours for rapid and delayed) to the masses of 2M05215658+4359220 and its dark companion reported by T18 (black points). We also highlight the BH-GS binaries with $P_{\text{orb}}/\text{day} = 83.2 \pm 50$ and $e = 0$ with colored points. The over-density of simulated systems having $M_{\text{GS}}/M_{\odot} \gtrsim 2$ is dominated by binaries formed within the last 1.5 Gyr where the GS companion at present is undergoing core helium burning in most cases, with a few on the first giant branch or asymptotic giant branch. Systems with lower GS masses are dominated by binaries that formed between 1.5 and 10 Gyr ago with GS companions on the first giant branch.

Both derived masses from T18 are broadly consistent with the results of our simulations. The wider constraints placed without using $\log g$ measurements (triangle marker in Figure 4) are consistent with both populations created using rapid and delayed SN models. However, the tighter constraints placed by imposing a $\log g$ measurement (circle marker in Figure 4) are inconsistent by $> 3\sigma$ with all BH-GS binaries from our rapid model.

If we restrict our attention to systems with $P_{\text{orb}}/\text{day} = 83.2 \pm 50$, we find that the wider mass constraints allow BH-GS binaries with first giant branch, asymptotic giant branch, or core helium burning GS companions for both SN engine models. However, the tighter mass constraints allows only GS companions that are either undergoing core helium burning or are on the asymptotic giant branch. Our results therefore suggest that

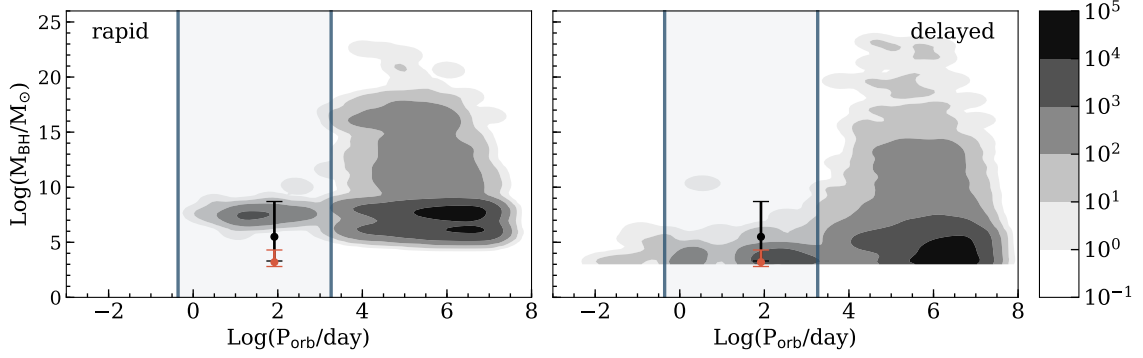


Figure 3. Distribution of P_{orb} vs BH mass resulting from the rapid (left) and the delayed SN prescription (right). The lower limit on the BH mass is set to $3 M_{\odot}$ in our binary evolution models. Contours show the expected BH-GS number in the MW. Black and orange points show the observed $P_{\text{orb}}/\text{day} = 83.2$ and the two derived masses for the BH provided by T18. The shaded blue region shows a guideline for P_{orb} to which *Gaia* is sensitive; the upper limit is set by *Gaia*'s 5 yr mission duration and the lower limit is set to 0.5 day based on the average minimum P_{orb} resolvable by *Gaia* (Breivik et al. 2017).

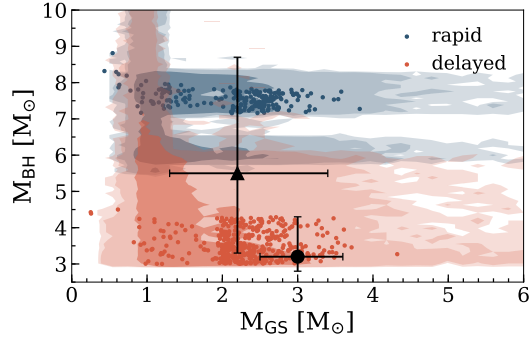


Figure 4. Shaded regions show the 1σ , 2σ , and 3σ distributions of BH mass vs GS mass for BH-GS binaries for the delayed (orange) and rapid (blue) SN prescriptions. The points of the same colors denote the same for a sub-population satisfying $P_{\text{orb}}/\text{day} = 83.2 \pm 50$ (Section 3.2). The black error bars show limits on the BH and GS masses derived in T18, the lower (circle) and higher (triangle) estimates denote derivations by T18 with and without a $\log g$ measurement.

future observations of 2M05215658+4359220 will help place strong constraints on the evolutionary state of the GS. Furthermore, combining a strong constraint on GS mass with an astrometrically resolved orbit will allow a precise constraint on the BH mass and thus probe both BH formation models and the BH mass gap.

4. DISCUSSION

4.1. *Gaia* detectability

As mentioned by T18, the orbit of 2M05215658+4359220 will produce an angular oscillation of $\sim 0.2 \text{ mas}$ for a nominal distance of 3.7 kpc and combined binary mass of $7 M_{\odot}$. The current *Gaia* position uncertainty on this system is $\sim 0.05 \text{ mas}$, which should improve to $\sim 0.03 \text{ mas}$ after five years of observations, suggesting that *Gaia* will be able to astrometrically resolve the

orbit of 2M05215658+4359220 by at least a factor of a few. Furthermore, within *Gaia* DR2 (22 months of observations) 2M05215658+4359220 has been observed 25 times. Extrapolating forward, we can expect > 60 observations of the system during the nominal five-year *Gaia* mission, implying the orbit will be well-observed.

We note that the orbital motion of the binary ($\sim 0.2 \text{ mas}$) is a sizable fraction of the parallax that *Gaia* measures for 2M05215658+4359220 (0.272 mas), making the current parallactic distance unreliable. This complicates the interpretation of 2M05215658+4359220. The case of HR 6046, a 5th magnitude star in a six-year orbit with an unknown companion, provides a demonstrative example. The parallax to HR 6046 was measured by *Hipparcos*; however, Torres (2007) showed that this estimate was unreliable and the parallactic motion, proper motion, and astrometric motion all needed to be simultaneously fit to obtain an accurate distance. With the simultaneous fit as well as literature RV measurements, Torres (2007) completely solved the orbit of HR 6046, measuring the component masses to a precision better than $0.1 M_{\odot}$.

It has long been recognized that *Gaia* will detect the astrometric motion of certain binary stars (e.g., Jancart et al. 2005), and indeed, the identification and fitting of binary star orbits is a dedicated task handled by the Coordination Unit 4 within the *Gaia* collaboration (Eyer et al. 2013). With the inclusion of binary stars in the third data release of *Gaia* (expected in 2021), an astrometric and radial velocity determination of the orbit for 2M05215658+4359220 is therefore imminent.

4.2. X-ray Luminosity Puzzle

GSs lose mass in winds, which BH companions can accrete. Following the prescription outlined in Belczynski et al. (2008) for Bondi-Hoyle-Littleton wind accretion, we can derive the X-ray luminosity (L_X) expected from a particular BH-GS binary. For instance, if we place the

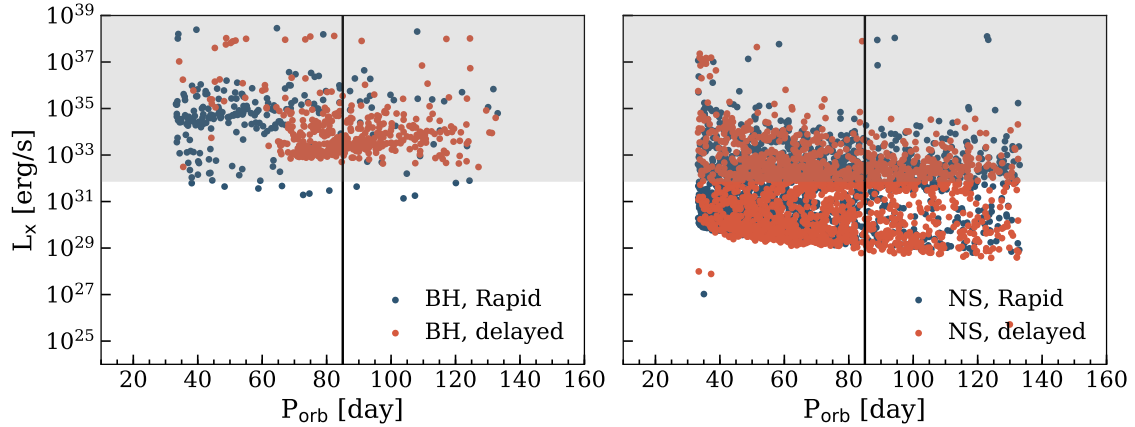


Figure 5. L_X vs P_{orb} expected from the accretion of the GS wind by the BH for our sub-population of binaries similar to 2M05215658+4359220 (see Section 4 for details). The majority of our simulated BH-GS binaries (left) produce L_X higher than the upper limit of $\sim 10^{32} \text{ erg s}^{-1}$ from T18. However, the X-ray upper limit is consistent with certain NS accretors (right).

well-studied star α Boo (Arcturus; which has properties similar to the giant star in 2M05215658+4359220), using its wind mass loss rate and wind velocity, in an 83.2-day orbit with a $3 M_\odot$ BH, we derive $L_X \sim 10^{35} \text{ erg s}^{-1}$, nearly four orders of magnitude higher than the X-ray upper limit of $7.7 \times 10^{31} \text{ erg s}^{-1}$ calculated from the *Swift* non-detection by T18.

To further investigate this, we simulated a population of NS-GS binaries as described in Section 2, and applied the accretion formalism of Belczynski et al. (2008) to our simulated BH-GS and NS-GS binaries. Figure 5 shows L_X vs P_{orb} for our simulated BH-GS and NS-GS binaries with orbital periods within 50 days of 2M05215658+4359220. The left panel shows that the vast majority BH-GS binaries in our specified P_{orb} range produce L_X above the X-ray upper limit (indicated by the grey region). Alternatively, the right panel of Figure 5 shows that our simulated NS-GS binaries produce substantially lower L_X , making most of them compatible with the *Swift* non-detection. Furthermore, the relatively low accretion rates may place NS-GS systems within the propeller regime (Illarionov & Sunyaev 1975; Ghosh & Lamb 1979), leading to even lower L_X than our simplified estimates suggest.

While these results seem to suggest that the L_X upper limit is inconsistent with a BH accretor, we note that a subset of accreting BHs (albeit in systems with very different properties from 2M05215658+4359220) have quiescent luminosities $< 10^{32} \text{ erg s}^{-1}$, which are explained using advection-dominated accretion flow models (Garcia et al. 2001). Furthermore wind accretion in binaries is a notoriously difficult problem (Theuns et al. 1996; de Val-Borro et al. 2017) that is complicated by clumping (Bozzo et al. 2016), small-scale instabilities (Manousakis & Walter 2015), and the back reaction of accretion luminosity onto the donor star’s atmosphere (Sander et al. 2018). Thus the non-detection of X-rays from

2M05215658+4359220 is not sufficient to put constraints on the nature of the unseen companion. However, the X-ray upper limits make 2M05215658+4359220 an interesting case study for testing wind accretion models and finding the nature of the compact companion.

5. CONCLUSION

We have shown that BH-GS binaries similar to 2M05215658+4359220 are naturally produced in binary population synthesis simulations for the MW. While several formation channels produce BH-GS binaries, the dominant formation channel for circular BH-GS binaries in short-period orbits similar to 2M05215658+4359220 requires evolution through a CE.

We find that the mass of the BH is a direct consequence of the SN-engine model used. Thus, a strong constraint on the mass of the remnant companion to 2M05215658+4359220 could help to constrain models for the SN engine and BH formation. If 2M05215658+4359220’s companion is confirmed to be a BH with $M_{\text{BH}}/M_\odot \sim 3$, for example, by the next *Gaia* data release, the existence of the BH mass gap, and the rapid SN-engine model can be ruled out altogether. These constraints have wide reaching implications for predictions of BH binaries observed using radio, X-ray, and GWs.

Finally, we introduced a tension between the non-detection of X-rays from 2M05215658+4359220 by *Swift* and standard wind accretion theory for our population of BH-GS binaries. *Gaia*’s next data release, expected in mid 2021, is certain to improve the constraints on the mass of 2M05215658+4359220 and its dark companion and shed light on several of these mysteries.

K.B. is grateful to Astrid Lamberts for assistance with accessing the Latte simulation suite. J.J.A. acknowledges funding from the European Research Coun-

cil under the European Union's Seventh Framework

Programme (FP/2007-2013)/ERC Grant Agreement n. 617001.

REFERENCES

- Abbott, B. P., Abbott, R., Abbott, T. D., et al. 2016, *Physical Review Letters*, 116, 061102
- Abbott, B. P., Abbott, R., Abbott, T. D., et al. 2016, *Physical Review Letters*, 116, 241103
- Abbott, B. P., Abbott, R., Abbott, T. D., et al. 2017, *Physical Review Letters*, 118, 221101
- Abbott, B. P., Abbott, R., Abbott, T. D., et al. 2017, *ApJL*, 851, L35
- Abbott, B. P., Abbott, R., Abbott, T. D., et al. 2017, *Physical Review Letters*, 119, 141101
- Abt, H. A. 1983, *ARA&A*, 21, 343
- Barstow, M. A., Casewell, S. L., Catalan, S., et al. 2014, *arXiv:1407.6163*
- Belczynski, K., Kalogera, V., Rasio, F. A., et al. 2008, *ApJS*, 174, 223
- Belczynski, K., Wiktorowicz, G., Fryer, C. L., Holz, D. E., & Kalogera, V. 2012, *ApJ*, 757, 91
- Bond, H. E., Schaefer, G. H., Gilliland, R. L., et al. 2017, *ApJ*, 840, 70
- Bozzo, E., Oskina, L., Feldmeier, A., & Falanga, M. 2016, *A&A*, 589, A102
- Breivik, K., Chatterjee, S., & Larson, S. L. 2017, *ApJL*, 850, L13
- Burrows, A., Vartanyan, D., Dolence, J. C., Skinner, M. A., & Radice, D. 2018, *SSRv*, 214, 33
- Chatterjee, S., Rodriguez, C. L., & Rasio, F. A. 2017, *ApJ*, 834, 68
- Claeys, J. S. W., Pols, O. R., Izzard, R. G., Vink, J., & Verbunt, F. W. M. 2014, *A&A*, 563, A83
- Corral-Santana, J. M., Casares, J., Muñoz-Darias, T., et al. 2016, *A&A*, 587, A61
- de Val-Borro, M., Karovska, M., Sasselov, D. D., & Stone, J. M. 2017, *MNRAS*, 468, 3408
- Eyer, L., Holl, B., Pourbaix, D., et al. 2013, *Central European Astrophysical Bulletin*, 37, 115
- Farr, W. M., Sravan, N., Cantrell, A., et al. 2011, *ApJ*, 741, 103
- Fryer, C. L., Belczynski, K., Wiktorowicz, G., et al. 2012, *ApJ*, 749, 91
- Gallo, E., Miller-Jones, J. C. A., Russell, D. M., et al. 2014, *MNRAS*, 445, 290
- Garcia, M. R., McClintock, J. E., Narayan, R., et al. 2001, *ApJL*, 553, L47
- Ghosh, P., & Lamb, F. K. 1979, *ApJ*, 234, 296
- Giesers, B., Dreizler, S., Husser, T.-O., et al. 2018, *MNRAS*, 475, L15
- Heggie, D. C. 1975, *MNRAS*, 173, 729
- Hobbs, G., Lorimer, D. R., Lyne, A. G., & Kramer, M. 2005, *MNRAS*, 360, 974
- Hopkins, P. F. 2015, *MNRAS*, 450, 53
- Hopkins, P. F., Wetzel, A., Kereš, D., et al. 2018, *MNRAS*, 480, 800
- Hurley, J. R., Tout, C. A., & Pols, O. R. 2002, *MNRAS*, 329, 897
- Illarionov, A. F., & Sunyaev, R. A. 1975, *A&A*, 39, 185
- Jancart, S., Jorissen, A., Babusiaux, C., & Pourbaix, D. 2005, *A&A*, 442, 365
- Kroupa, P. 2001, *MNRAS*, 322, 231
- Lamberts, A., Garrison-Kimmel, S., Hopkins, P. F., et al. 2018, *MNRAS*, 480, 2704
- Manousakis, A., & Walter, R. 2015, *A&A*, 575, A58
- Mashian, N., & Loeb, A. 2017, *MNRAS*, 470, 2611
- Masuda, K., & Hotokezaka, K. 2018, *arXiv:1808.10856*
- Mazeh, T., Goldberg, D., Duquennoy, A., & Mayor, M. 1992, *ApJ*, 401, 265
- Messenger, C., & Veitch, J. 2013, *New Journal of Physics*, 15, 053027
- Özel, F., Psaltis, D., Narayan, R., & McClintock, J. E. 2010, *ApJ*, 725, 1918
- Sander, A. A. C., Fürst, F., Kretschmar, P., et al. 2018, *A&A*, 610, A60
- Theuns, T., Boffin, H. M. J., & Jorissen, A. 1996, *MNRAS*, 280, 1264
- Thompson, T. A., Kochanek, C. S., Stanek, K. Z., et al. 2018, *arXiv:1806.02751*
- Trimble, V. L., & Thorne, K. S. 1969, *ApJ*, 156, 1013
- Torres, G. 2007, *AJ*, 134, 1916
- van Haften, L. M., Nelemans, G., Voss, R., et al. 2013, *A&A*, 552, A69
- Vink, J. S., de Koter, A., & Lamers, H. J. G. L. M. 2001, *A&A*, 369, 574
- Wetzel, A. R., Hopkins, P. F., Kim, J.-h., et al. 2016, *ApJL*, 827, L23
- Woosley, S. E. 2017, *ApJ*, 836, 244
- Yalinewich, A., Beniamini, P., Hotokezaka, K., & Zhu, W. 2018, *MNRAS*, 481, 930
- Yamaguchi, M. S., Kawanaka, N., Bulik, T., & Piran, T. 2018, *ApJ*, 861, 21